BioGecko

Vol 12 Issue 03 2023
ISSN NO: 2230-5807

ANALYSIS OF SWITCHED RELUCTANCE MOTOR FOR LAPAROSCOPIC APPLICATIONS

Dr. Indira S
Assistant Professor, Department of Electronics,
Sri Ramakrishna College of Arts & Science (Autonomous),
Coimbatore, Tamil Nadu, India
Email: indiras1987@gmail.com

Abstract

Cancer is a disease that creates panic among people due to its vicious and incurable nature. Cancer research is one of the most essential and challenging areas of focus in the medical field. Hormone therapy, targeted therapy, radiotherapy, immunotherapy, and chemotherapy are the available cancer treatment modes. Hence better treatment and detection means to detect and cure cancer at the early stage is required. However, undergoing the surgery will differ according to the patient based on the patient's health, type of cancer and type of surgery. The current era is that of minimally invasive surgery that has been extended to cancer in the form of laparoscopic surgery. Motors are used to control the operation of instrument in Laparoscopic surgery. In both industrial and home applications, the switched reluctance motor (SRM) is becoming more popular. It has numerous advantages, including robustness, lossless excitation, low maintenance, a large speed range, great dependability, and a wide working temperature range. The significant torque ripple is a major disadvantage of SRM. High torque ripple causes vibration, noise, and reduces the motor's overall performance. Torque ripple has a significant effect near low speeds, while its effect at high speeds is very minor due to strong momentum. To improve the motor's performance, it's critical to reduce the torque ripple. The reduction of SRM torque ripple is now a study area. Because of its doubly prominent nature, SRM has a built-in torque ripple. With suitable design improvements and enhanced control procedures, torque ripple can be eliminated. The goal of this work is to reduce torque ripple through design changes. It is only recently that tremendous developments in power electronics drive technologies have made adjustable speed drives with Switched Reluctance Motor a huge success.

Keywords: *Laparoscope, SRM*

1.1 Introduction

The SRM drive is gaining in popularity among electric drives due to its simple, sturdy structure, low production cost, fault tolerance capability, and high efficiency. It also has several drawbacks, such as the need for electronic control and a shaft position sensor, and the noise and torque ripple caused by the double salient construction. SRMs are often created with the goal of maximizing converter rating use. Because this machine can work in a continuous switching mode, the word "switched" comes to mind. Second, the word reluctance enters the picture since both the stator and the rotor are made up of variable reluctance magnetic circuits, or we could say it has a doubly significant structure.

SRM control cannot be compared to either the alternating current motor or the direct current motor, which are both fed with sinusoidal current waveforms. Square current waveforms can be employed in the simplest control since each motor phase (winding) must be magnetized and demagnetized at the proper moments of rotor position. However, because the motor is very non-linear, the electromagnetic torque is determined not only by the instantaneous current amount but also by a non-linear inductance profile, implying that using simply square current waveforms will result in torque with a significant ripple component.

SRMs often lack magnets in the rotor and stator, resulting in a construction that is simple, inexpensive, and stable. In some versions of these motors, however, a small amount of permanent magnetic materials is utilised to boost torque. The stator poles to rotor poles ratios used in SRMs are very limited, with the most frequent being 4:6 and 6:8, each with its own set of multipliers. It's worth noting that each phase is made up of two coils facing each other. As a result, the stator will have three phases for 4:6 and four phases for 6:8 ratios, respectively.

1.2 CONSTRUCTION AND OPERATION OF SRM

Silicon steel stampings with inward projecting poles make up the stator. The stator's number of poles can be an even or an odd number. The majority of available motors have an even number of stator poles (6 or 8). Field coils are attached to all of these poles. Phase windings are formed by connecting the field coils of opposing poles in sequence so that their MMFs are additive. Phase windings are made up of a single coil or a series of coils. The motor's terminal is connected to each of the phase windings. These terminals are wired to the output terminals of a power semiconductor switching circuitry with a D.C. supply as an input.

The rotor is made up of silicon steel stampings with outwardly protruding poles as well. The number of poles on the rotor differs from the number on the stator. The number of rotor poles in most available motors is 4 or 6, depending on the number of stator poles, which can be 6 or 8. A position sensor is mounted on the rotor shaft. The signals collected from the rotor position sensor influence the turning ON and turning OFF operations of the various devices in the power semiconductor circuits. The block diagram of SRM is shown in Figure 4.1. The power semiconductor switching circuitry, which is coupled to various phase windings of the SRM, receives a dc supply.

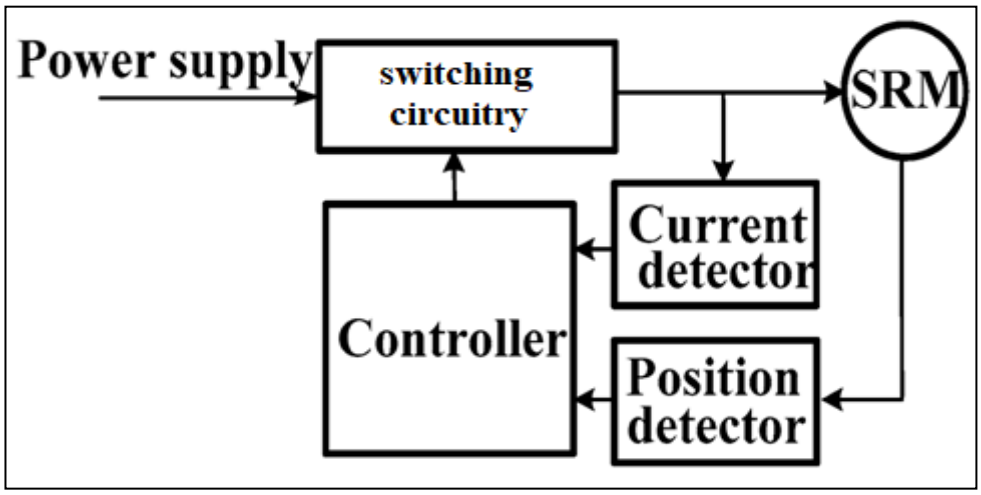

Figure 1.1 Block Diagram of SRM motor

The rotor position sensor, which is positioned on the SRM shaft, sends signals to the controller concerning the rotor's position in relation to the reference axis. The controller takes this data, as well as the reference speed signal, and appropriately switches on and off the power semiconductor device connected to the dc supply. The current signal is also given back to the controller, which uses it to keep the current within safe limits.

1.3 CONTROL TECHNIQUES

Various control techniques have been developed primarily for the purpose of reducing torque ripple and increasing efficiency. These can be classified into three categories: voltage impulse control, maintaining a constant current, and maintaining a constant torque.

1.3.1 Voltage impulse control

The SRM's simplest controller is the impulse control. It's mostly utilized for high-speed control and systems that don't require a lot of driving performance. A speed controller, a phase control technique, a block that generates transistor signals, and an over current safeguard are all part of the usual implementation architecture shown in Figure 4.

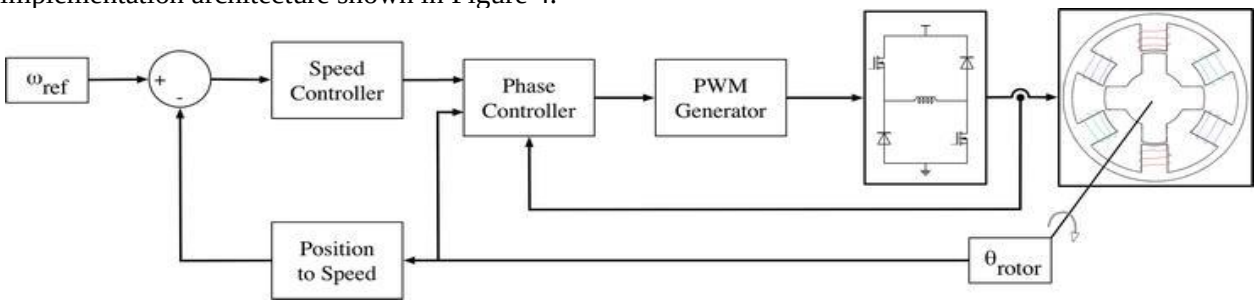

Figure 1.2 Speed control loop based on impulse control

A linear PI controller is typically utilized as the speed controller, as it is in other electric drives with other electrical machines. It receives the speed error and outputs a voltage reference signal. Phase control is responsible for activating each phase and determining how the reference voltage should be applied. In order to provide effective control, it is critical to have high precision in rotor position measurement.

1.3.2 Current control

In the controller, the voltage is kept constant, and the current is assumed to remain constant as well. This does not happen due to back-EMF and varied inductance levels for different rotor positions. As a result, a current controller for each phase is required to overcome this constraint**.**

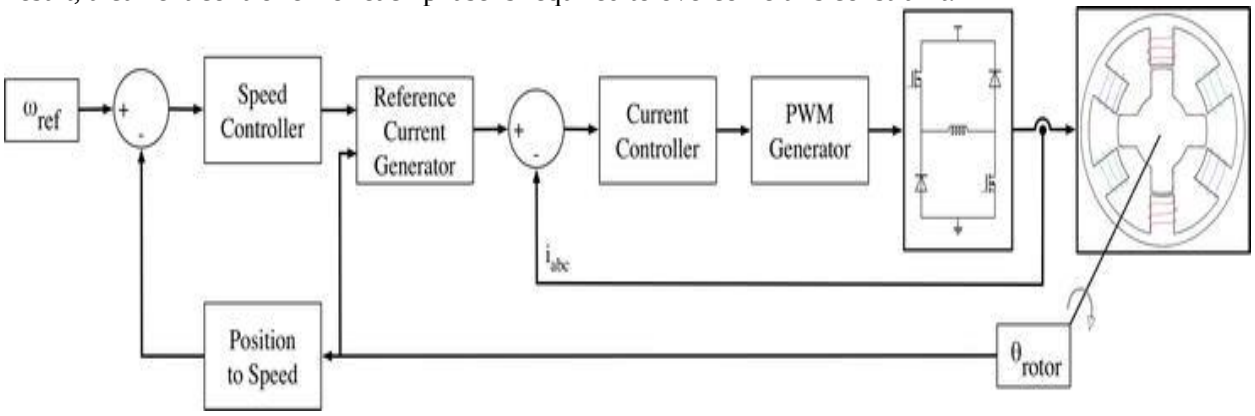

Figure 1.3 Block diagram of speed control based on current control

This controller's configuration, as illustrated in Figure 4.3, is cascaded, with the current regulated in the inner loop and the speed controlled in the outer loop. In addition, depending on the rotor position, a decision block determines whether each phase must conduct current or not.

1.3.3 Torque control

One of the key goals of a speed controller is to maintain consistent torque with the least amount of ripple as feasible. For most applications, using a sensor to measure instantaneous torque is too costly.

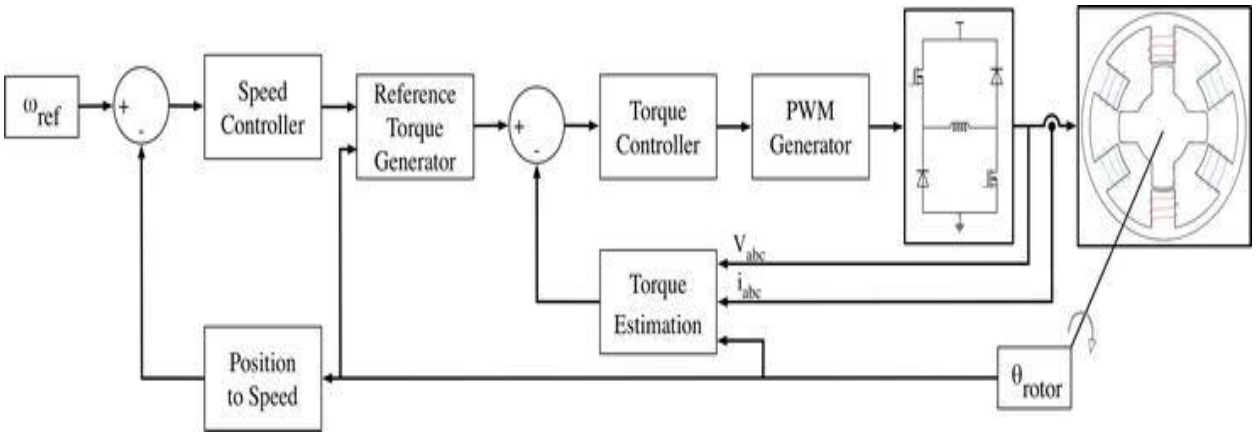

Figure 1.4 Torque control diagram

1.4.4 Mathematical Equation of SRM

The application of DITC's mathematical equations to SRM is explored here. The voltage across the motor winding at any given time is given by:

$$v = Ri + \frac{d\psi(\theta,i)}{dt} \quad (1)$$

where ψ(θ, i) is the phase flux-linkage, which is a function of rotor position θ and current i.
Thus, the equation for the power flow can be written as:

$$vi = Ri^2 + i\frac{\partial\psi(\theta,i)}{\partial i}\frac{di}{dt} + i\frac{\partial\psi(\theta,i)}{\partial\theta}\frac{d\theta}{dt} \quad (2)$$

$$dW_m = i\frac{\partial\psi(\theta,i)}{\partial\theta}d\theta - \frac{\partial W_f}{\partial\theta}d\theta \quad (3)$$

where, dWm and dWf are the differential mechanical energy and field energy, respectively.
The instantaneous torque is defined by:

$$T = \frac{dW_m}{d\theta} \quad (4)$$

The expression for the instantaneous torque production of an SRM phase can be written as:

$$T = i\frac{\partial\psi(\theta,i)}{\partial\theta} - \frac{\partial W_f}{\partial\theta} \quad (5)$$

This is a rarely used variant of conventional torque equation. Due to saturation in the SRM, the influence of the second term in Eq. (5) is negligible. Therefore, by using this approximation, the following equation for torque production may be obtained as:

$$T \approx i\frac{\partial\psi(\theta,i)}{\partial\theta} \quad (6)$$

1.5 Results and discussions

A 12 V DC supply voltage is employed. Over the speed range, the converter turn-on and turn-off angles are kept constant at 45 degrees and 75 degrees, respectively. The hysteresis band is set to + -10 A and the reference current is 20 A. The SRM is begun by connecting the regulator input to the step reference. The rate of acceleration is determined by the properties of the load. A relatively light load was chosen to reduce the start time. Because just the currents are controlled, the motor speed will grow in accordance with the system's mechanical dynamics.

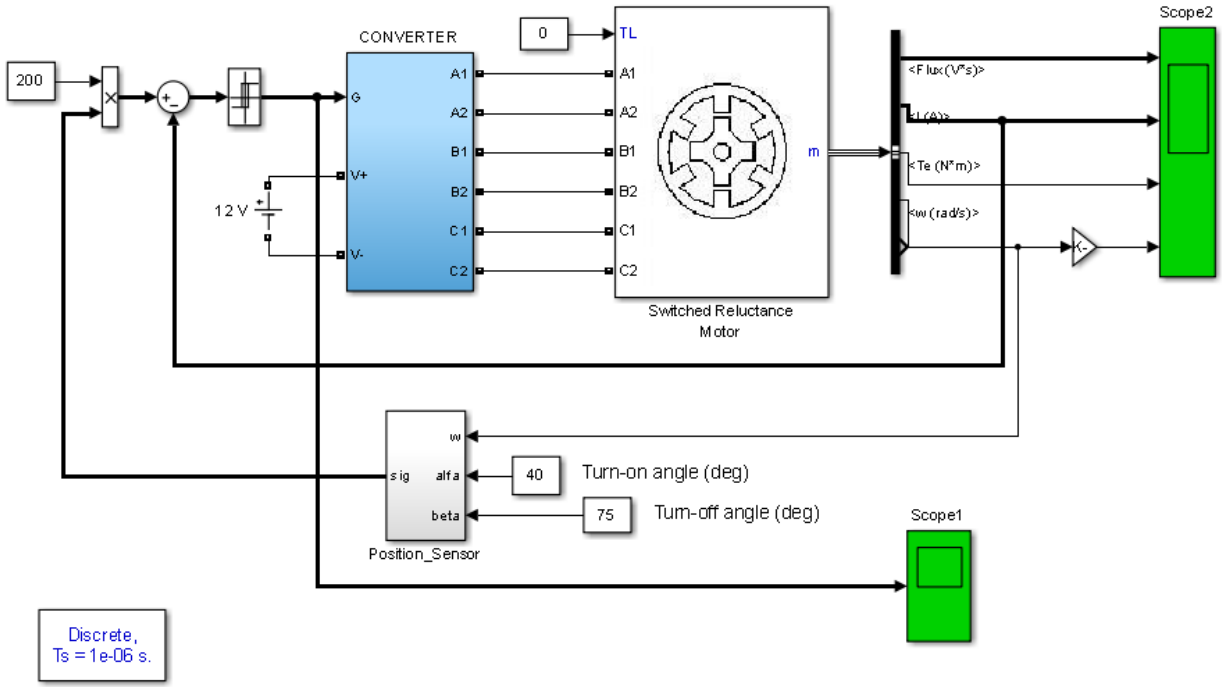

Figure 1.5 Simulation diagram of proposed system

The motor's EMF is low from standstill to around 3000 rpm, allowing the current to be controlled to the reference value. The average value of the created torque is approximately proportional to the present reference in this operation mode. We also note the torque ripple caused by the hysteresis regulator switching, in addition to the torque ripple caused by phase transitions. This method of operation is also known as continuous torque operation.

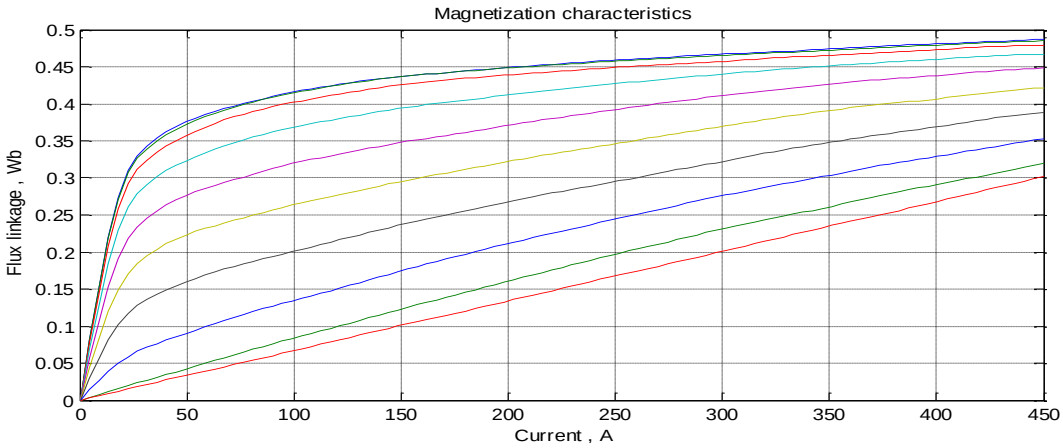

Figure 1.6 SRM Magnetization Characteristics

Figure 4.6 shows the magnetization characteristics of the Switched Reluctance Motor. It shows the magnetizing properties like flux linkage in Webbers with respect to Current rating. From the graph says that the different characteristics wave form.

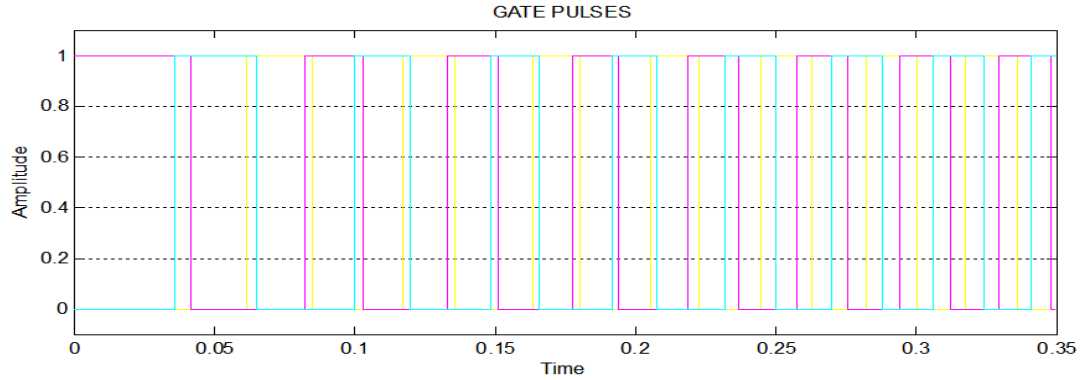

Figure 1.7 Control pulses for SRM driver

The motor's EMF is high at speeds above 3000 rpm, and the phase currents cannot reach the current regulators' reference value. The converter automatically converts to voltage-fed mode, with no manipulation of the power switches. During their active periods, they remain closed, and a constant DC supply voltage is provided to the phase windings. As can be seen on the scope, this results in linearly varying flux waveforms. The SRM acquires its 'natural' characteristic in voltage-fed mode, where the average value of produced torque is inversely proportional to motor speed.

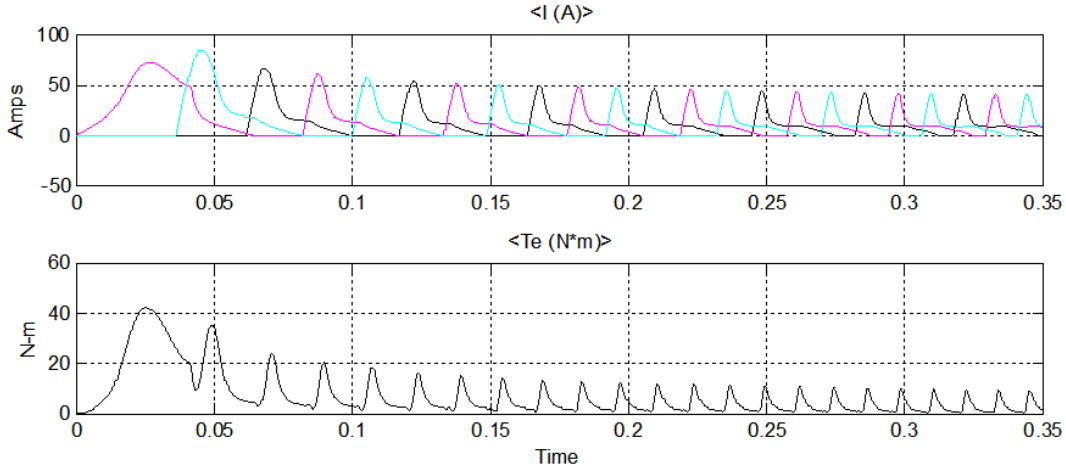

Figure 1.8 SRM motor torque output

The average torque and torque ripple in SRM drives are influenced by the turn-on and turn-off angles, as well as the current waveforms in the motor phases. And these qualities alter as the motor speed increases. In many applications, such as electric vehicle drives, the highest torque/ampere ratio and lowest torque ripple are highly desirable, and this over the widest speed range conceivable. Applying applicable pre-calculated turn-on and turn-off angles in function of the motor current and speed can optimise the SRM torque characteristic. A 2-D lookup table can be used to hold the optimum values of optimum angles.

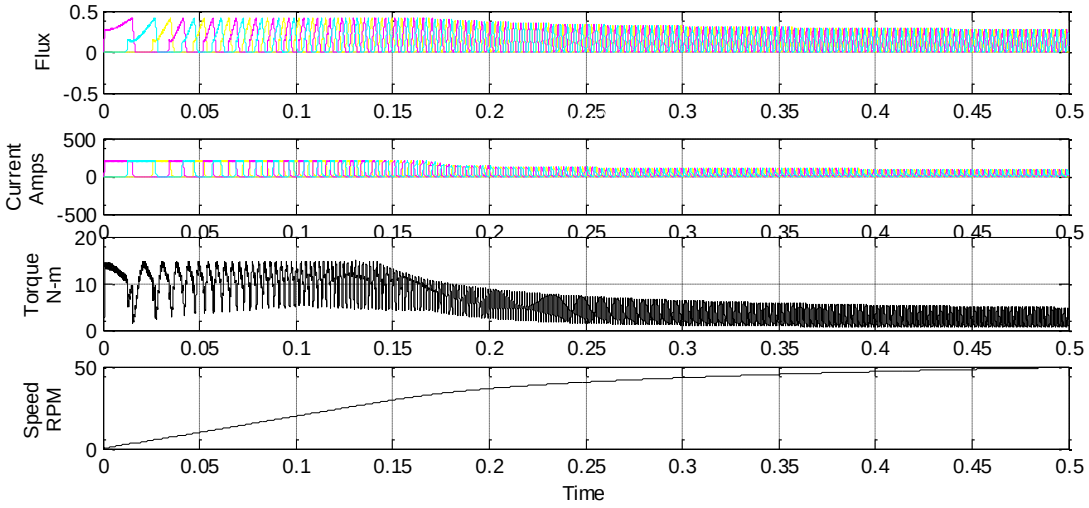

Figure 1.9 SRM Flux output corresponding Operation

Figure 1.9 shows the Switched reluctance motor flux output of stator, current rating of stator during operation, the motor torque rating based on the rotor speed in RPM. The speed at starting gradually increases and for a certain time period rotor speed reaches to the desired speed.

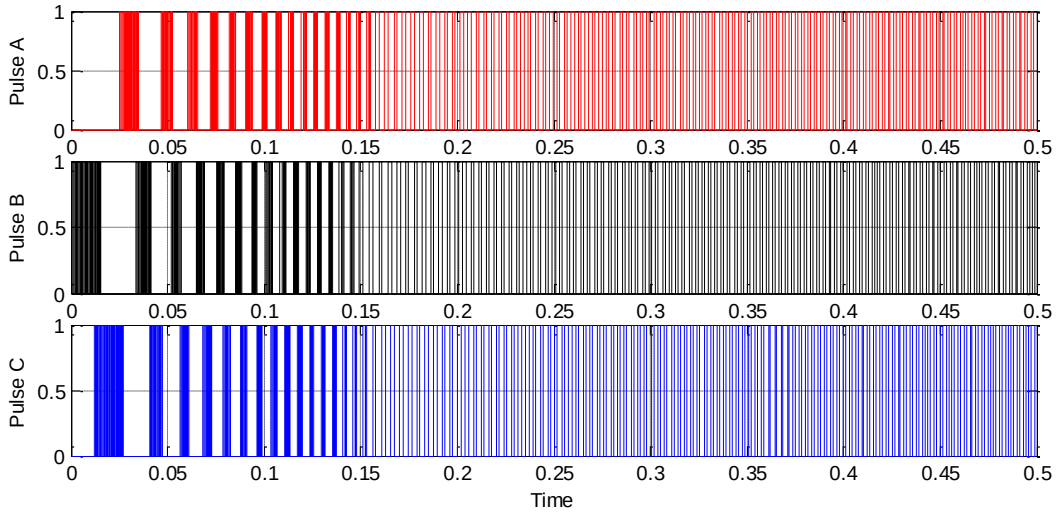

Figure 1.10 Control pulses for SRM stator phases

Figure 1.10 shows the pulse output for three phases like SRM stator. in this SRM motor having 6 poles in stator side and also 4 poles in rotor side. The pulse patterns are shown here.

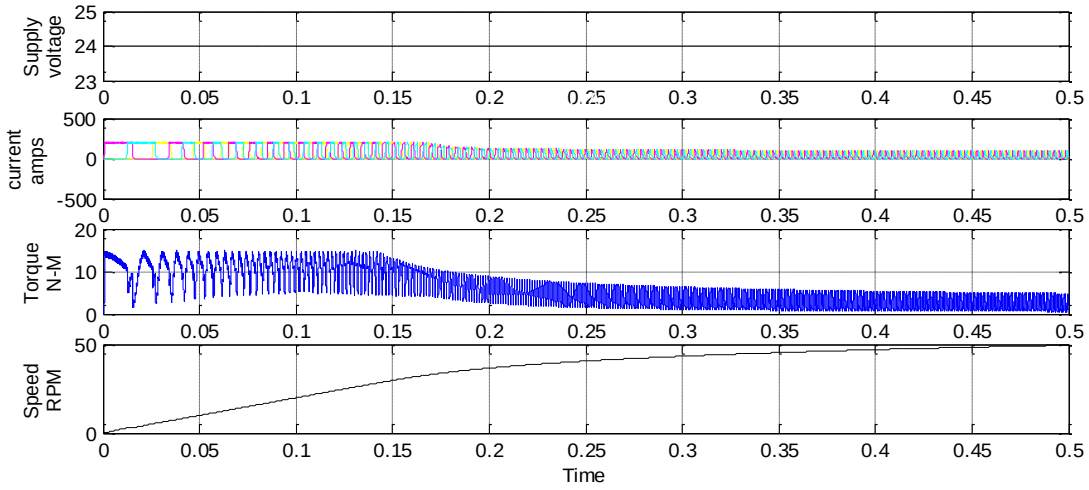

Figure 1.11 SRM motor supplied by 24 V

Figure 1.11 shows that the output characteristics of SRM when supplied with a DC voltage of 24V. Based on the input voltage, the motor power rating will not change. The motor takes current like 30 Amps rating in three phases in order to meet the power ratings. The torque is 5 N-M during stable condition, at starting the motor taking maximum torque for picking up the speed. the speed of the rotor reaches 50 RPM from 0 RPM.

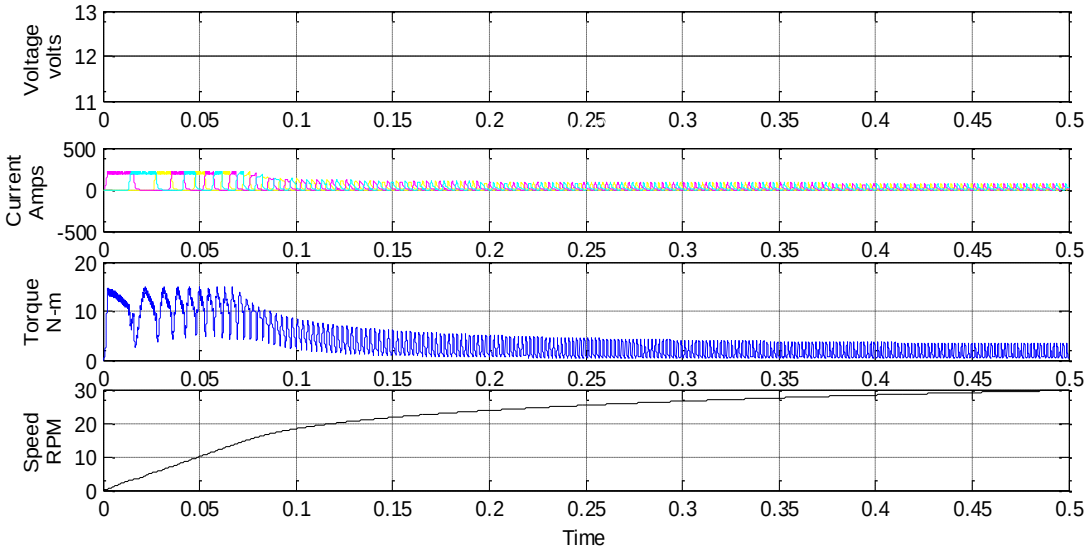

Figure 1.12 SRM motor supplied by 12 V

Figure 1.12 show that the output characteristics of SRM while supplying the DC voltage of 12V. Based on the input voltage, the motor power rating will not change. The motor takes current like 35 Amps rating in three phases in order to meet the power ratings. The torque is 5 N-M during stable condition, at starting the motor taking maximum torque for picking up the speed. The speed of the rotor reaches 30 RPM from 0 RPM.

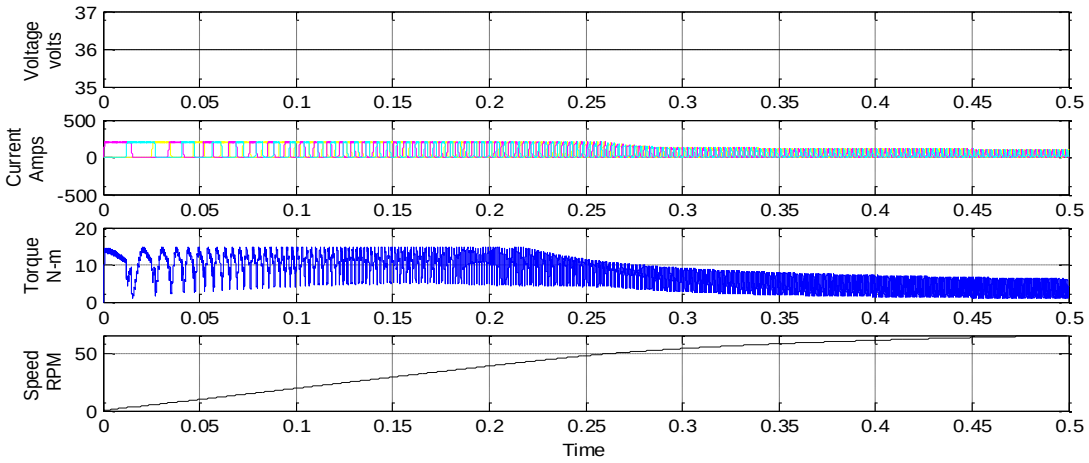

Figure 1.13 SRM motor supplied by 36 V

Figure 1.13 shows the output characteristics of SRM while supplying the DC voltage of 12V. based on the input voltage, the motor power rating will not change. The motor takes current like 36 Amps rating in three phases in order to meet the power ratings. The torque is 5 N-M during stable condition, at starting the motor taking maximum torque for picking up the speed. The speed of the rotor reaches 65 RPM from 0 RPM.

1.6 CONCLUSION

The features of the SRM in continuous and discontinuous conduction mode are examined in this research. The SRM control parameters were tuned in order to maximize output power. The optimal control parameters, as well as the accompanying torque, power, and efficiency, were defined as functions of motor speed for both modes of operation. When the acquired findings for these two modes of operation are considered and compared, it can be determined that continuous mode can deliver much higher SRM power at high rotational speeds.

REFERENCES

1. International Agency for Research on Cancer (IARC): World Cancer Report: Cancer Research for Cancer Prevention 978-92-832-0448-0 (2020).
2. Pollack LA, Rowland JH, Crammer C, Stefanek M: Introduction: charting the landscape of cancer survivors' health-related outcomes and care. Cancer 2009; 115: 4265-4269
3. Howe, James R., Nipun B. Merchant, Claudius Conrad, Xavier M. Keutgen, Julie Hallet, Jeffrey A. Drebin, Rebecca M. Minter et al. "The North American Neuroendocrine Tumor Society Consensus Paper on the Surgical Management of Pancreatic Neuroendocrine Tumors." Pancreas 49, no. 1 (2020): 1-33.
4. Louie, Brian E., Jennifer L. Wilson, Sunghee Kim, Robert J. Cerfolio, Bernard J. Park, Alexander S. Farivar, Eric Vallières, Ralph W. Aye, William R. Burfeind Jr, and Mark I. Block. "Comparison of video-assisted thoracoscopic surgery and robotic approaches for clinical stage I and stage II non-small cell lung cancer using the Society of Thoracic Surgeons database." The Annals of thoracic surgery 102, no. 3 (2016): 917-924.
5. Hall, Eric J. "Intensity-modulated radiation therapy, protons, and the risk of second cancers." International Journal of Radiation Oncology* Biology* Physics 65, no. 1 (2006): 1-7.
6. Dawson, Laura A., and David A. Jaffray. "Advances in image-guided radiation therapy." Journal of clinical oncology 25, no. 8 (2007): 938-946.

7. S. Sung, J. Lee and I. Lee "Process identification and PID control," (John Wiley & Sons).
8. H. Shin and J. Park, "Anti-Windup PID Controller with Integral State Predictor for Variable-Speed Motor Drives," IEEE Transactions on Industrial Electronics, vol.59, no.3, pp. 1509–1516, 2012.
9. S. Pandey, P. Dwivedi and A. Junghare, "A Newborn Anti-Windup Scheme Based on State Prediction of Fractional Integrator for Variable Speed Motor," IEEE 17th Int. Conf. on Control, Automation and Systems (Ramada Plaza Jeju Korea), pp. 663−668, 2017.
10. F. Padula, A. Visioli and M. Pagnoni, "On the Anti-Windup Schemes for Fractional-Order PID Controllers," IEEE Int. Conf.on Power Electronics, Intelligent Control and Energy Systems (Delhi India) pp. 1−4, 2012.
11. S. Pandey, P. Dwivedi and A. Junghare, "Anti-Windup Fractional Order PIλ−PDμ Controller Design for Unstable Process: a Magnetic Levitation Study Case Under Actuator Saturation," Springer Arabian Journal for Science and Engineering vol. 42, no. 12, pp. 5015–5029, 2017.
12. A Mehrabian and C. Lucas, "A Novel Numerical Optimization Algorithm Inspired from Weed Colonization," Ecological informatics, vol.1, no.4, pp. 355–366, 2006.
13. S. Mekni and B. Fayech, "A Modified Invasive Weed Optimization Algorithm for Multi-Objective Flexible Job Shop Scheduling Problems," Computer Science & Information Technology, pp. 51–60, 2014.
14. M. Khalilpour, N. Razmjooy, H. Hosseini and P. Moallem, "Optimal Control of DC Motor Using Invasive Weed Optimization (IWO) Algorithm," Majlesi Int. Conf. on Electrical Engineering (Iran), January 2011.
15. B. Nayak and S. Sahu, "Parameter Estimation of DC Motor through Whale Optimization Algorithm," International Journal of Power Electronics and Drive System (IJPEDS), vol. 10, no. 1, pp. 83-92, 2019.
16. P. Acarnley, Stepping Motors: A Guide to Modern Theory and Practice, 4th ed. London, U.K.: The Institution of Engineering and Technology, 2002.
17. Q. N. Le and J.-W. Jeon, “Neural-network-based low-speed-damping controller for stepper motor with an FPGA,” IEEE Trans. Ind. Appl., vol. 57, no. 9, pp. 3167–3180, Aug. 2010.
18. Y. Anzai, S. Nishikata, and F. Tatsuta, “Studies on a sensorless initial rotor position estimating method for hybrid stepping motors,” in Proc. Int. Conf. Elect. Mach. Syst., Nov. 2009, pp. 1–4.
19. M. Boussak, “Implementation and experimental investigation of sensorless speed control with initial rotor position estimation for interior permanent magnet synchronous motor drive,” IEEE Trans. Power Electron., vol. 20, no. 6, pp. 1413–1421, Nov. 2005.
M. Bendjedia, Y. Ait-Amirat, B. Walther, and A. Berthon, “DSP implementation of rotor position detection method for hybrid stepper motors,” in Proc. Int. Power Electron. Motion Control Conf., 2006, vol. 3, pp. 1–3.
20. H. Gao, F. R. Salmasi, and M. Ehsani, “Inductance model based sensorless control of the switched reluctance motor drive at low speed,” IEEE Trans. Power Electron., vol. 19, no. 6, pp. 1568–1573, Nov. 2004.

21. N. Bianchi, S. Bolognani, J. Jang, and S. Sul, “Comparison of PM motor structures and sensorless control techniques for zero-speed rotor position detection,” IEEE Trans. Power Electron., vol. 22, no. 6, pp. 2466–2475, Nov. 2007.
22. J. Hu, J. Liu, and L. Xu, “Eddy current effects on rotor position estimation and magnetic pole identification of PMSM at zero and low speeds,” IEEE Trans. Power Electron., vol. 23, no. 5, pp. 2565–2575, Sep. 2008.